Light rays and imaging in wave optics

Władysław Żakowicz

Institute of Physics, Polish Academy of Sciences, Al. Lotników 32/46, 02-668 Warsaw, Poland

An interpretation of focusing and image formation on scattering of electromagnetic waves by a dielectric cylinder (a cylindrical lens) is proposed on the basis of the full Maxwell theory. It is centered on analysis of the behavior of integral curves of the Poynting vector here called wave rays. These wave rays cannot intersect so that the focusing and imaging spots are identified with regions of high flow concentration. Two-dimensional examples of wave rays and wave fronts in the scattering of plane and cylindrical electromagnetic waves as well as of Gaussian beams by a dielectric cylinder derived from rigorous solution of the Maxwell equations for incident waves perpendicular to and uniform along the scatterer are given. Their qualitative comparison with geometrical and diffraction approximations are provided. Fixed points and vortex structure of the Poynting flow are investigated. An example of (Gaussian-beam) scattering with transparent multiple internal reflections and multiple wave splitting is given.

I. INTRODUCTION

This paper attempts to discuss wave propagation and focusing effects with the help of exactly solvable problem of classical electrodynamics of the scattering of an electromagnetic wave by a lossless perfect dielectric cylinder. The monochromatic electromagnetic fields that are used satisfy exactly the corresponding Maxwell equations with all necessary boundary conditions.

Formation and properties of optical images in optical systems belong to the most extensively studied problems of classical electrodynamics. Elementary geometrical-optics theory, based on the ray tracing methods, describes the light focusing and formation of images of illuminated objects using few rules of rectilinear propagation of rays in uniform media and simple laws of refraction and reflection at different media interfaces. This very simple theory is not only able to explain the basic principles of most optical instruments but also, in its more developed form, enables one to deal with distortions and aberrations of optical systems. Discussions of these problems can be found in all books on optics, in particular, one can refer to the monographs by Born and Wolf [1] and Sommerfeld [2]. Mathematical aspects of geometrical-optics are discussed in [3] while numerous examples of applications can be found in [4].

Beside purposely achieved focusing and imaging, the light very often exhibits unintended or "natural" focusing properties occurring in various forms of conspicuous bright lines and spots in reflected or transmitted light. In the frame of geometrical-optics and ray tracing methods these distinguished effects correspond to caustics, i.e., envelopes of bunches of rays that are basically smooth and stable with the exception of certain points at which they change their pattern in discontinuous way forming cusps. The range of such very common effects has been systematically covered within catastrophe theory by Nye [5].

To define the rays in theories based on wave physics first an eikonal, defined as an optical path and closely related to the phase of the wave, has been introduced by Sommerfeld and Runge [6] and discussed in [1,2]. The rays are identified with lines that are tangent to the gradient of the eikonal at each point. It is to be noted that the concept of eikonal is strictly connected with the short-wave approximation in optics and diffraction theory. The eikonal approximation can be useful in analysis of light propagation in weakly nonuniform media. At first, the concept of eikonal had been introduced for scalar waves this scalar function were applied in a full vector wave theory based on Maxwell's equations [1,3].

Although our discussion is restricted to the electromagnetic wave propagation problems described by Maxwell equations many properties of these problems occur in other wave theories. The most important example is quantum or wave mechanics. Just as the eikonal approximation was proposed to link wave optics with geometrical optics, so the hydrodynamic approximation to the Schrödinger equation was proposed, as early as in the beginnings of quantum theory [7], to link wave functions with classical trajectories.

However, these asymptotic theories are insufficient if the geometrical rays are intersecting. In the geometrical optics, the definition of intensity of light at a given point is determined by its distance from the center of curvature of the wave front passing through this point [8]. The centers of curvature of the wave fronts lie on surfaces, which according to [8], can be identified with caustics. Therefore, at the points lying on the caustics the intensity becomes infinite, and thus can be determined only by wave theory. Geometro-optical foci themselves are distinguished points forming cusps of the caustics. To deal with the apparent singularities of intensity on caustics and foci, better theories, which take into account the wave properties of radiation are necessary.

Wave properties of light, not restricted by the short-wave approximation, are usually considered within diffraction theories. These theories started with the Huygens principle, while later findings of Young and Fresnel led to the Huygens-Fresnel formulation followed by the Kirchhoff and Kirchhoff-Helmholtz diffraction integral representation. These early formulations of the diffraction theory were carried out for scalar waves. The generalizations to the vector wave fields have been discussed in [9–12].

Quantitative applications of these diffraction theories are

difficult as the solutions are given in terms of integrals of rapidly oscillating functions and thus many special functions were defined and asymptotic methods of "steepest descent" (called also "stationary phase" or "saddle points" methods) were developed. The dominant contribution to the integrals can be evaluated by deformation of the integration contour in the complex plane. In addition, the diffraction integrals methods require the knowledge of field distribution on some reference surface. Very often "a reasonable guess" could provide this distribution or it could be derived using a geometrical-optics approach. The geometrical-optics approach was applicable in multicomponent optical systems in which the diffraction-based calculations were restricted to the last stage of wave beam propagation. The comparison of various diffraction approximations, presentation of computational methods in the studies of focusing problems have been discussed by Stamnes [13].

As mentioned above, diffraction problems lead to expressions containing various complicated integrals. Severe difficulties in computation of these integrals were overcome, in particular, by Pearcey [14] still before computers were really available.

Different properties of the diffraction integrals, usually studied with the help of stationary phase methods, were connected with various image patterns and interpreted in the frame of catastrophe theory [15,5,16]. The wave fronts derived in these diffraction-based theories exhibit phase singularities at points or along lines where the wave amplitude vanishes. Nye and Berry compared these singularities with dislocations occurring in crystals [17]. This paper stimulated discussions of many optical effects, e.g., airy rings in the wave diffracted by a circular aperture, in terms of wave dislocations [18,19]. The relations of phase singularities and dislocations of waves with geometrical rays, caustics, and catastrophes are presented in [16].

The observed optical phenomena are so complex and rich that approximate theories to describe them become very complicated. Many approximations have only a limited range of applicability and any claims for universality are rather problematic. Therefore, the desire a solvable diffraction model has been expressed many times, e.g., [13,5,20,21]. In this context, Mie's scattering [1] of a plane wave by a dielectric sphere was mentioned most often. In fact, Khare and Nussenzveig [22] attempted to apply rigorous Mie approach to the rainbow theory. They found, however, an extremely fine structure of solutions, rapidly changing with the sphere radius, as well as the necessity of taking, for their parameters, several thousand partial waves. Thus, that approach was not recommended any further. Instead, approximate but analytical summation of partial waves contribution, based on the Watson transformation, was considered advantageous [23]. However, this analytical approach leads to an extremely complicated formalism involving functions analytically extended into the complex plane of complex angular momenta, as well as complex wave vector k, and still is only approximated as it requires data on the reflection and transmission coefficients of Debye terms.

The problem studied in this paper is similar to the Mie problem as the solution is expressed in the form of partial-wave expansion. However, it is simpler since the cylindrical partial waves are simpler than the spherical ones, and selecting incident waves to be normal to and uniform along the cylinder the configuration chosen can be completely described on a two-dimensional (2D) plane.

The scattering of plane electromagnetic waves by a dielectric cylinder was treated for the first time by Lord Rayleigh [24] and has long been of great theoretical interest as it admits exact solution (see, e.g., [25] for a more recent reference). This solution can be written in terms of partial waves that can be expressed in terms of the well known Bessel functions. With the present state of the art computations this solution can be handled with almost arbitrary precision. While most papers dealing with scattering on a cylinder consider the incident field to be a plane wave, similar methods can be used to describe the scattering of waves emitted from well-localized sources placed in the vicinity of the cylinder and for incident Gaussian beams [26–28]. A linear long antenna placed near an infinite cylinder, while being a highly idealized source of isotropic cylindrical wave, provides the simplest model of a point source located near a lens. In particular, it allows for a reconstruction of the image formation from the point of view of the rigorous Maxwell theory. Let us notice that the solvability of the model has been utilized in [29] where the complete system of solutions to the Maxwell equations has been determined and applied to the field quantization and description of spontaneous emission from an atom located near the cylinder.

The present paper attempts to provide an interpretation of the image formation within the framework of the rigorous Maxwell theory without explicit reference to traditional optical interpretations based either on geometrical optics or even supplemented by wave-optics effects including diffraction and the Huygens principle. That does not mean that the traditional interpretations of optical phenomena are incorrect, however, it may be of some interest to show how the electromagnetic fields themselves deal with very rich optical phenomena.

In this work we only consider incident waves that are perpendicular to the cylindrical scatterer axis (taken as the z axis of the Cartesian or cylindrical coordinate system). In addition, we assume that the incident waves are uniform along the cylinder. With these two assumptions the general scattering problem simplifies to the two-dimensional problem with the relevant field components dependent on the x and y variables and the Poynting vector field remaining in the x-y plane.

Wave-optical rays associated with the transport of energy are consequently defined as integral curves of the field of (time-averaged) Poynting vector and show how the images are formed by focusing of rays. In fact, such energy flow lines were introduced by Braunbek and Laukien [30] (in their investigation of the diffraction by a half-plane) and by Boivin, Dow, and Wolf [11], in their study of a focused beam. The second analysis was restricted to the focal region only and the fields were evaluated within the diffraction approximation. In the present model the wave light rays can be derived for the entire space including the interior of the optical system (cylindrical lens in this case).

A simple consequence of mathematical properties of the differential equations describing the light wave rays is the exclusion of the ray intersections as well as their division and termination except at absorbers, conductors, and particular discrete (for a given finite cylinder radius) set of trajectories, discussed further.

Wave fronts or equiphase surfaces are represented in the present simple 2D model by curves in the x-y plane orthogonal to the set of wave rays. This set of equiphase curves, wave fronts, can be derived from a set of differential equations similar to that for the rays.

Both sets of equations for light rays and wave fronts distinguish certain characteristic points. At these points the time-averaged Poynting vectors vanish. A more detailed discussion of these stationary points is given in Sec. IV D. In particular, there are stationary points of "vortex" type, in the vicinity of which the Poynting flow circulates and equiphase lines are attracted, and those of "saddle point" type that in generic cases repel both integral curves. Some very specific rays can either terminate at the "saddle points," or, starting at these points, run to infinity or, forming a loop, return back to the same "saddle point." These critical curves specify separatrices isolating Poynting flows of different types. The generic wave light rays can either start at the source and run to infinity or form a close vortex line. The existence of closed Poynting flows is an important property of the electromagnetic radiation flux. Such lines occur very often in shadow regions forbidden for the geometrical rays and are important for the descriptions of radiation beam splitting and intersection of two separate beams.

In the framework of quantum scattering theory the integral curves tangent to the quantum current field, called streamlines, were proposed in [31] to illustrate fluid features of the wave function in the scattering process. The scattering of plane scalar waves by spherical potential wells and barriers were considered. Although the scatterers were three-dimensional spheres the axial symmetry of scattering reduced this discussion to the 2D problem. The formation of the streamlines vortices were shown. However, the scatterers were rather small and not too many partial waves were necessary. Therefore, many characteristic optical features discussed in the present paper were not present.

The vortex-type fixed points in the theories that take the wave fronts as principal objects correspond to singular points of phase. However, there is nothing singular in these points when the fields are taken as fundamental variables.

In contrast to the light rays that in the generic cases are indestructible, the equiphase lines can terminate and start at the vortex points. The number of fixed points strongly depends on the radius of the cylinder, the position of the light source, and on the type of incident beam. Perhaps the abundance of such points for the system investigated in [22] caused the rapid variation of the scattered radiation pattern.

As was noticed in [32,19,18] the structure of the focus was partly influenced by diffraction effects at the aperture boundaries or stops supporting the focusing lenses. For unsupported lenses and for Gaussian-beam illumination the focusing patterns simplify. Similar features have been found in the investigated system for the incident Gaussian beam with the width smaller than the cylinder diameter. For such beams the rays propagate very smoothly through the lens. All stationary points are shifted outside the incident beam. In this case one can find the reflected rays going back to the half-space of the incident beam. There were no such reflected rays in the other two cases, i.e., those of incident plane wave or incident cylindrical wave. For the plane-wave illumination, all rays seem to flow to the forward direction and one can ask what happened with evidently present backscattering. Backscattered rays can emerge only at the wings of the Gaussian beams where the usually weak scattered wave is not dominated ("overshined") by the much stronger incident beam. When a Gaussian beam with nonzero "impact parameter" is applied, several internal reflections are visible and can be studied in detail. Nussenzveig's [20] classes of multiple-reflected and refracted rays can be easily identified and interpreted as scattered bundles of wave rays in our 2D scattering model. This result makes it possible to interpret the 2D analogue of rainbow within the framework of wave optics in a Cartesian-like way.

The rest of the paper is organized as follows. Section II defines the mathematical models and contains the basic equations. Section III is devoted to the presentation of the global properties of wave rays and the comparison with the standard geometrical-optics picture of ray propagation through a lens. The discussion of the fine structure of rays and equal-phase contours as well as of fixed points is provided in Sec. IV. An investigation of rays and stationary points specifically for the case of Gaussian-beam illumination is given in Sec. V. Section VI demonstrates the behavior of intensity and phase along the optical axis. The problem of image formation of extended objects is elucidated in Sec. VII by analysis of radiation of two point sources near a cylinder. Section VIII is devoted to the multiple internal reflections and refractions of rays by and inside the lens. Section IX contains several final remarks.

II. THE MODEL AND ITS SOLUTION

In this work we consider the problem of scattering of an incident $\mathbf{E}^{inc}$ stationary wave (dependent on time as $e^{-i\omega t}$) propagating in the x-y plane and with such polarization that the electric field is orthogonal to this plane. The waves are scattered by a dielectric infinite cylinder of radius a. The dielectric is assumed to be homogeneous, lossless, and nondispersive. Its refraction index is n_d. We place the origin of the cylindrical coordinate system in the center of the cylinder with the z axis directed along the cylinder. In this case the whole electromagnetic field is determined from the E_z component of the electric field. The magnetic field stays in the x-y plane.

The electromagnetic field outside the sources is described by the Helmholtz equation

$$\nabla^2 E_z(r,\phi) + n^2(r)k^2 E_z(r,\phi)$$

$$= \left(\frac{\partial^2}{\partial r^2} + \frac{1}{r}\frac{\partial}{\partial r} + \frac{1}{r^2}\frac{\partial^2}{\partial \phi^2} + n^2(r)k^2 \right) E_z(r,\phi) = 0,$$

$$(1)$$

where $k=\omega/c$, $n(r)=n_d$ for $r<a$, and $n(r)=1$ for $r>a$. The solution of Eq. (1) can be written as

$$E_z(r,\phi)=E_z^{inc}(r,\phi)+\sum_{m=-\infty}^{\infty}b_m e^{i\phi m}H_m^{(1)}(kr),\quad r>a$$

$$E_z(r,\phi)=\sum_{m=-\infty}^{\infty}a_m e^{i\phi m}J_m(n_d kr),\quad r<a,\qquad(2)$$

where J_m denote the Bessel functions of the first kind and order m, while $H_m^{(1)}$ is the Hankel functions of the first kind and order m.

Three different incident waves corresponding to a source at infinity, an infinitely long and infinitely thin linear antenna at finite distance from the cylinder, and a Gaussian beam, are considered in this paper. The electric fields in these three cases, expressed in terms of partial cylindrical waves, are as follows:

I. Plane-wave propagating in the $\mathbf{k}(\alpha)=k\{\cos\alpha,\sin\alpha,0\}$ direction

$$E_z^{inc}(\mathbf{r})=E_0 e^{i\mathbf{k}\cdot\mathbf{r}}=\sum_{m=-\infty}^{\infty}i^m J_m(kr)e^{im(\phi-\alpha)}.\qquad(3)$$

II. Cylindrical wave emitted by an antenna placed at $\mathbf{r_0}$ or $\{r_0,\phi_0\}$ if polar coordinates are used

$$E_z^{inc}=AH_0^{(1)}(k|\mathbf{r}-\mathbf{r_0}|)$$
$$=AH_0^{(1)}[k\sqrt{r^2+r_0^2-2rr_0\cos(\phi-\phi_0)}],\qquad(4)$$

$$E_z^{inc}(r,\phi)=AH_0^{(1)}(k|\mathbf{r}-\mathbf{r_0}|)$$
$$=A\sum_{m=-\infty}^{\infty}J_m(kr)H_m^{(1)}(kr_0)e^{im(\phi-\phi_0)},$$
$$r<r_0.\qquad(5)$$

III. Gaussian beam

$$E_z^{inc}(\mathbf{r})=E_0\int d\alpha P(\alpha)e^{i\mathbf{k}(\alpha)\cdot(\mathbf{r}-\mathbf{r_0})}$$
$$=E_0\sum_{m=-\infty}^{\infty}i^m J_m(kr)e^{im\phi}\int d\alpha P(\alpha)e^{-im\alpha}e^{-i\mathbf{k}(\alpha)\cdot\mathbf{r_0}},$$
$$(6)$$

where $P(\alpha)=(w/\sqrt{\pi})e^{-w^2\alpha^2}$, $\mathbf{r_0}$ is the position of the beam waist, and w is the width of the beam waist (also specifying its angular spread, $\mathbf{\Delta}=1/w$).

The coefficients a_m and b_m are determined by the continuity conditions of the tangent electric (E_z) and magnetic fields ($H_\phi\propto\partial_r E_z$) at the boundary of the cylinder. These amplitudes are equal to

$$a_m=\mathcal{G}_m\frac{J_m'(ka)H_m^{(1)}(ka)-J_m(ka)H_m^{(1)'}(ka)}{n_d H_m^{(1)}(ka)J_m'(n_d ka)-J_m(n_d ka)H_m^{(1)'}(ka)},$$
$$(7)$$

$$b_m=\mathcal{G}_m\frac{J_m'(ka)J_m(n_d ka)-n_d J_m(ka)J_m'(n_d ka)}{n_d H_m^{(1)}(ka)J_m'(n_d ka)-J_m(n_d ka)H_m^{(1)'}(ka)},$$
$$(8)$$

where in the three cases considered here we have

$$\mathcal{G}_m=E_0 i^m e^{-im\alpha},\quad\text{plane wave,}$$

$$\mathcal{G}_m=Ae^{-im\phi_0}H_m^{(1)}(kr_0),\quad\text{cylindrical wave,}\qquad(9)$$

$$\mathcal{G}_m=E_0 i^m\int d\alpha P(\alpha)e^{-i\mathbf{k}(\alpha)\cdot\mathbf{r_0}}e^{-im\alpha}\quad\text{Gaussian beam.}$$

A small simplification may be achieved in Eq. (7) by noting that the numerator contains the Wronskian of the J_m and $H_m^{(1)}$ functions.

Finding the solution for the electric field one can immediately get the corresponding magnetic field

$$H_x=-\frac{i}{\omega\mu_0}\frac{\partial E_z}{\partial y},\quad H_y=\frac{i}{\omega\mu_0}\frac{\partial E_z}{\partial x},\quad H_z=0,$$

and the time-averaged Poynting vector field: $\langle\mathbf{S}\rangle=\frac{1}{2}\operatorname{Re}e\mathbf{E}\times\mathbf{H}^\star$.

In the case of a Gaussian beam the incident wave E_z^{inc} and the expansion coefficients for the cylindrical partial $\mathcal{G}_m$ require the integration over the angles α. While for a given beam and cylinder configuration all relevant partial-wave expansion coefficient $\mathcal{G}_m$ must be calculated only once and the scattered part of the wave can be evaluated as fast as in the other two cases, the fields of the incident wave require α integration at each position point $\mathbf{r}$. This leads to some inconveniences when one looks for light rays. To avoid these inconveniences two computational approximations can be made. In the first one the beam is represented by a finite number of plane waves with $\alpha_j=j\Delta/N_e$, $\{j=-N_e,-N_e+1,\ldots,N_e-1,N_e\}$. The second approximation is valid for beams that are not very narrow and therefore characterized by very small angular spread. In this case one can include only the quadratic expansion terms in $\mathbf{k}(\alpha)\approx\{1-\frac{1}{2}\alpha^2,\alpha,0\}$ and all integrations with the Gaussian distribution function $P(\alpha)$ can be done analytically. Thus, one gets

$$E_z^{inc}(x,y)\approx E_0\frac{2w}{\sqrt{4w^2+2ik(x-x_0)}}e^{ik(x-x_0)}$$
$$\times\exp\left(-\frac{k^2(y-y_0)^2}{4w^2+2ik(x-x_0)}\right),\qquad(10)$$

$$\mathcal{G}_m\approx E_0 i^m\frac{2w}{\sqrt{4w^2-2ikx_0}}e^{-ikx_0}\exp\left(-\frac{(m+ky_0)^2}{4w^2-2ikx_0}\right).$$
$$(11)$$

Light rays in the theory based on the Maxwell equations can be defined as the lines tangential to the time-averaged Poynting vector. Such lines are sometime called "the energy flow lines" [1]. They can be determined from the solution to the equation

$$\frac{d\mathbf{r}^{lr}}{d\tau} = \langle \mathbf{S}[\mathbf{r}^{lr}(\tau)]\rangle. \qquad (12)$$

It is to be stressed that we *define* the wave-optical light rays as the integral curves of Eq. (12).

There exist specific points for which the time-averaged Poynting vector vanishes,

$$\langle \mathbf{S}(\mathbf{r}^{lr})\rangle = 0 \qquad (13)$$

so that $d\mathbf{r}^{lr}/d\tau = 0$ at these points. They are usually (in the theory of differential equations and dynamical systems) called stationary or fixed. They play a crucial role in the characterization of fields in an optical system.

The equal-phase manifolds are in fact two-dimensional surfaces. However, since our system is homogeneous along the cylinder (z) axis, we can restrict ourselves to the intersection of these surfaces with any plane for z = const. Such intersections define curves described by the following equation

$$\frac{d\mathbf{r}^{\phi}}{d\tau} = \hat{\mathbf{z}} \times \langle \mathbf{S}[\mathbf{r}^{\phi}(\tau)]\rangle. \qquad (14)$$

The curves specified above will henceforth be called the "equal-phase contours."

III. GLOBAL STRUCTURE OF LIGHT RAYS: COMPARISON WITH GEOMETRICAL OPTICS

Although the expressions provided in Sec. II give the analytical solutions to the electromagnetic field scattering problem, they are fairly complicated and require numerical treatment for more specific exposure of the results. In particular, such numerical treatment is necessary to find solutions of Eq. (12) that are used to draw the lines tangent to the Poynting vector interpreted in this paper as wave light rays. The integrations have been performed using a routine based on the Runge-Kutta method with an automatically adjustable step (the Merson's scheme).

The Bessel functions were computed with the help of [33].

The number of terms in the field expansion necessary to reach the required accuracy depends basically on the width of the scattering cylinder and the separation of the wire antenna (line source) if this case is considered. Although the partial-wave expansion of fields in Eq. (2) runs formally from minus to plus infinity, for a fixed radius of the cylinder there is only a finite number N of terms for which the a_n and b_n coefficients take significant values. We estimate this critical number N to be $10a/\lambda$.

In our example of a dielectric cylinder of radius $a = 15\lambda$, the emitting antenna at $r_0 = 40\lambda$, and on using 2×150 (i.e., $-150 \leq m \leq 150$) partial waves the field continuity conditions are fulfilled with relative accuracy of 10^{-13}.

A. Comparison with geometrical optics

Figures 1 and 2 show the continuation of such light rays calculated as lines tangent to the Poynting vector and those
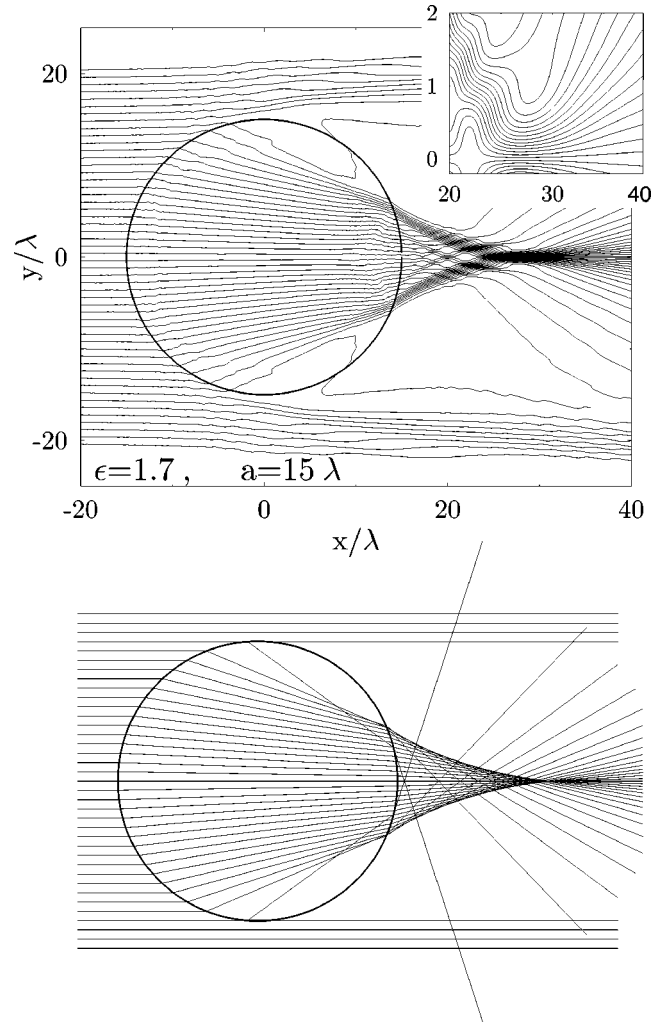
FIG. 1. Focusing of a plane wave by a cylindrical lens in wave and geometrical light ray optics. Normal wave incidence, $a = 15\lambda$, $n_d = \sqrt{1.7}$.

obtained according to the rules of geometrical optics. The light rays are sampled in such a way that the Poynting fluxes between the two consecutive rays passing through the lens are equal. In the case of an incident plane wave the starting points should be far to the left at equal Δy intervals. In the case of point antenna initial points for rays can be selected just as easily, since near this antenna radiation emission is isotropic.

One can find general agreement in the corresponding pictures, i.e., the incident plane wave is focused in the same regions and the wave emitted from the point source results in similar images. However, there are striking differences in both theories. The light rays defined according to the wave theory, being the integral curves of a continuous vector field, cannot cross each other (nor can any one of them cross itself, of course) as is shown in the top right segments of the presented figures. This property is completely different from the behavior of rays in geometrical optics. This observation leads to the reinterpretation of the image formation in wave optics.
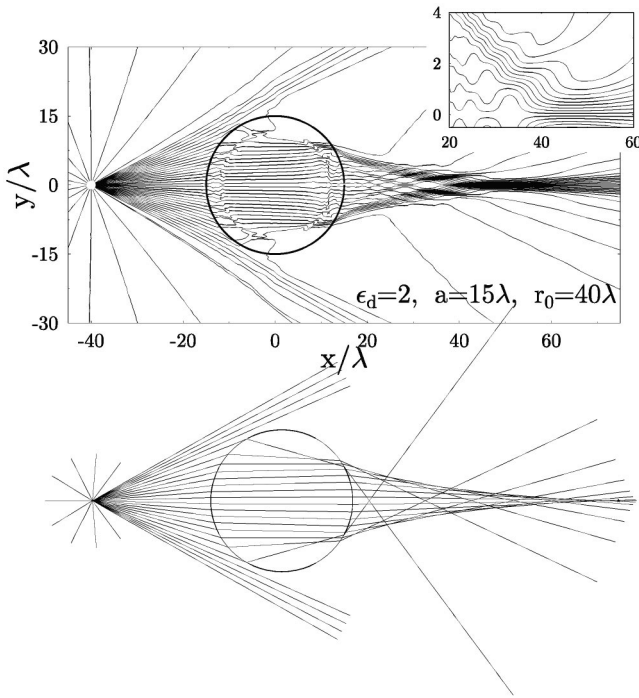
FIG. 2. Focusing and image formation of a cylindrical wave emitted at the distance r_0 from a cylindrical lens in wave and geometrical light ray optics. Normal wave incidence, $a = 15\lambda$, $n_d = \sqrt{2}$, $r_0 = 40\lambda$.

In wave optics the flow of electromagnetic flux as well as the density of the field energy become more dense in some regions of the space. Such regions, where the separations of light rays are very small, can be identified as the images of the sources located on the other side of the lens. The fact that the focus is not a point but a rather extended region in space is evident as well. There are some other differences between geometrical and wave rays.

One of the most ubiquitous and beautiful effects appearing in optical instruments are caustics, analyzed usually within the geometrical optics and/or theory of catastrophes [5,34,16]. In our pictures of the wave-optical rays, the caustics behind the cylinder are visible as well. They cannot be defined as the envelopes of bundles of crossing rays since the wave optical rays do not cross. The caustics appear, however, as the regions of enlarged density of rays at the boundaries of the beam of rays, see Figs. 1 and 2.

Near the boundaries and light concentration regions the wave light rays may become quite complicated, looking apparently erratic, though in geometrical optics the light should propagate along straight lines in homogeneous media. The wave ray flow approaching the focal region of image spot, with all its wiggles, is much different from the rather smooth departure flow. The behavior of fields in this region was intensively studied within diffraction-based theories starting from the numerical calculation of a diffraction integral performed by Pearcey and co-workers [14,34,5]. These results have usually been illustrated by drawing the magnitude and phase contours of the electric field. To compare our results with those earlier works, we include figures showing the contours of equal magnitude of the Poynting vector, see Figs.
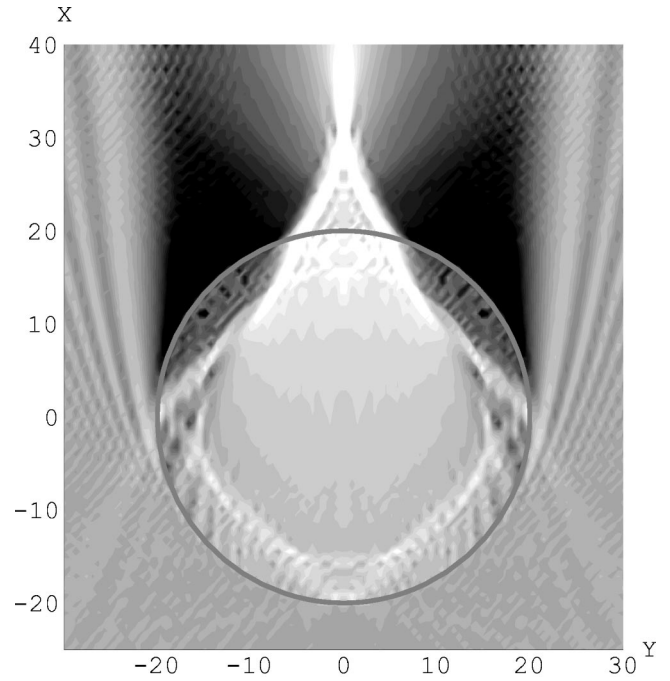
FIG. 3. Shaded contour plot of constant modulus of the Poynting vector $|S|$ (contours themselves are removed) for a cylinder $\epsilon = 2$, $a = 30\lambda$, and plane-wave illumination.

3 and 4. Figure 3 illustrates rather well the focusing properties of the cylindrical lens with the shadow region and bright and dark speckles distributed inside the lens along its boundary. A magnified part of Fig. 3 covering the focal region, together with an adjacent part of the lens is shown in Fig. 4. It evidently resembles analogous figures (as well as photographs) obtained with the help of the Pearcey integral and described as the cusp diffraction catastrophe shown in [34,15,5,16], although our approach does not use either diffraction integrals or any approximate diffraction theory at all.

Another interesting region is located near the boundaries where the rays approach the cylinder at grazing angles and groups of rays split into two bundles, one passing by the cylinder and the other one refracted by the lens. Our model allows for detailed study of the mechanism of this splitting process.

B. Rays in the shadow region

We observe that the beam of wave-optical rays splits itself in some regions close to the boundary of the cylinder. One set of rays enters the cylinder and is refracted, while another flows round the lens. Between these two parts there is a region of low intensity. (Both groups of rays eventually come again together at a large distance from the cylinder.)

The standard geometrical optics does not allow the rays to enter the shadow regions. However, from the solutions to the Maxwell equations it follows that there exist non-vanishing fields in these regions. The time-averaged Poynting vector is nonzero as well, and the wave-optical rays can be evaluated and studied.

Figure 5 shows a sample of several characteristic trajectories near the upper boundary of the lens where the ray-
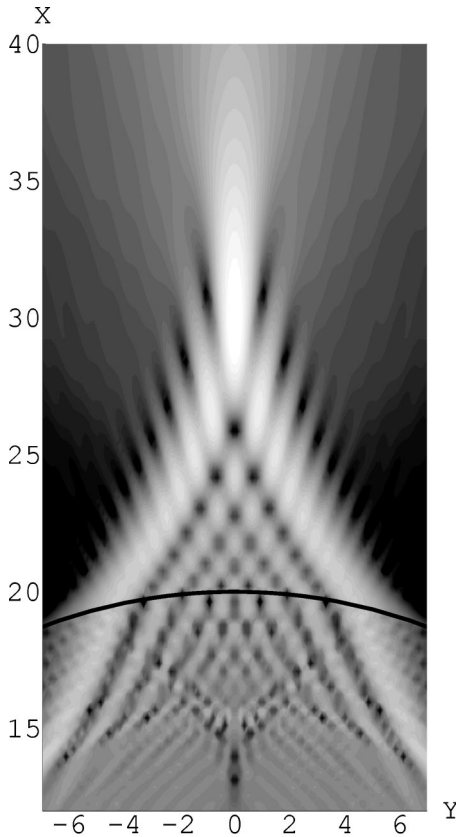
FIG. 4. Details of Fig. 3 in the focal and internal caustic region. Intensity pattern equivalent to a cusp diffraction catastrophe of [34] outside the cylinder lens is visible.

bundle splitting takes place. Some of these trajectories are clearly closed. There are other curves that, while starting at the source and going to infinity, meander and wind in a complex manner. The following section will be devoted to a detailed investigation and interpretation of such complex behavior.

Let us remark that in spite of sometimes erratic behavior of the flow lines mentioned above, the numerical integration is stable and on reversing the integration (i.e., performing it "back in time") one follows the same trajectory.

The flow lines can neither intersect, nor join nor split apart. The latter fact is a mathematical consequence of the unique dependence of solutions of a system of differential equations on initial conditions. Indeed, the vector field of the
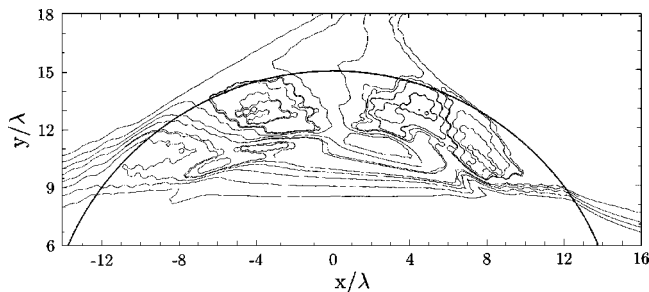
FIG. 5. Details of the upper part of Fig. 2 in the shadow region with families of meandering and bounded rays.
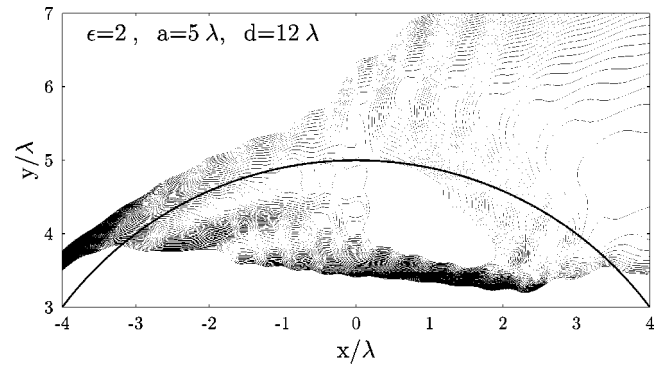
FIG. 6. Flow of an initially very dense bundle of rays—selected from all the rays emitted by the point source—in the shadow region; the overall picture of the bundle splitting and formation of void islands is provided; the parameters are $a=5\lambda$, $n_d=\sqrt{2}$, $r_0 =12\lambda$.

time-averaged Poynting vector is continuously differentiable (even real analytical) in the whole space except the boundary of the lens. Thus, it satisfies the Lipshitz condition. Therefore, the Picard theorem implies that the integral curves of the Poynting vector cannot intersect (cf., e.g., [35]). There are specific points—the saddle points of the phase—at which two or more wave-optical rays seem to meet. This does not mean, however, that the rays actually intersect. There is no possibility for one ray to reach a saddle point and to leave it. The saddle points cannot be reached by the wave-optical rays for any finite value of the parameter τ. There are rays that approach these points asymptotically to cross at $\tau \to \pm \infty$. (Such rays called separatrices will be more thoroughly studied below.) In other words, one might say that a trajectory attempting to cross itself at a point does not contain one piece only. There are at least two pieces that can join only for infinite pseudotime τ.

IV. PROPERTIES OF LIGHT RAYS, EQUAL-PHASE CONTOURS, AND FIXED POINTS

It is clear from Fig. 5 that the flow of rays can be very complicated. We may expect that the ray pattern becomes simpler for smaller radius of the cylinder. In what follows we shall consider in more detail a cylinder of the same refractive index but smaller radius to grasp more efficiently the essential properties of the light structure. The analysis of rays will be completed by investigation of equal-phase surfaces that are more frequently used in the studies of light propagation through optical instruments and other optical systems [1].

A. Islands in the stream of Poynting curves in the shadow region

For a cylinder with radius 5λ (i.e., three times smaller than in Fig. 5), we have plotted a very dense beam of rays (the source of light is still the line source) passing close to the boundary of the cylinder in Fig. 6. We observe the presence of "empty" or "white" islands with well-defined boundaries. They are inaccessible to the trajectories starting from the source. To investigate what happens in these islands
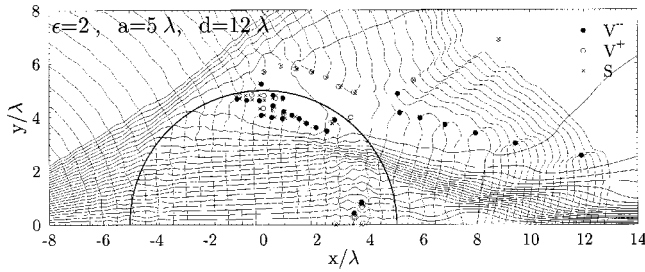
FIG. 7. Wave-optical rays (solid lines), equal-phase contours (dashed lines), and stationary points in the upper half-space for the same system as in Fig. 6.

we need to analyze additionally the equal-phase contours and the stationary points of the flow. Let us note that the equal-phase contours and stationary points are the very basic objects of important works dealing with the fine structure of light using the eikonal approximations and catastrophe theory [5].

In Fig. 7 the wave-optical rays and the equal-phase contours are plotted for the half-plane above the optical axis. The phase contours are obtained by integration of Eq. (14). It is clear that these contours (dashed lines) are perpendicular to the rays (solid lines), as should be the case. In the vicinity of the source they are almost circles, but in the cylinder and behind it, its form is very different and sometimes windy. We have started integration of Eq. (14) from the optical axis (in all cases we have checked that the phase along them is indeed constant, which has been another test of the accuracy of our solutions). It turns out that in many cases the integration terminates and it is not possible to continue it further. Starting integration from the top toward the bottom results in a similar termination of some contours at certain points. It is interesting that all the equal-phase curves starting in certain interval can terminate at the same point. We have found that such points are actually the stationary points of the flow defined by Eq. (13). Most of the stationary points are located in the regions empty of rays coming from the source. It is important, however, that in these regions the fields, the Poynting vector does not, in general, vanish and the phase is well defined with the exception of some points. Therefore, both the wave-optical rays and the equal-phase lines can be plotted. The structure of flows in the transient ("ray beam-splitting") region will be analyzed below.

B. Rays, phase contours, and fixed points for small lenses and line source—transient region

Figure 8 provides a picture of both unbounded and bounded rays in the transient region. The former ones start from the source and escape to infinity, although they wind and meander when passing through the transient region. Associated equal-phase contours and stationary points are also plotted.

Figure 8 indicates that the stationary points can be divided into two classes, the first one consists of the vortices (V) and the second one are the saddle points (S). We can also distinguish vortices that correspond to clockwise (V^+) and counter-clockwise (V^-) vortex flow. One can associate a to-
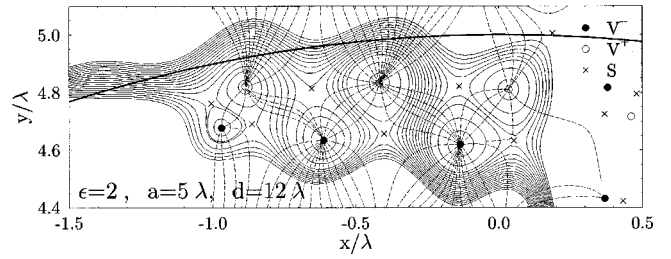
FIG. 8. Detailed structure of the flow in the bundle-splitting region for the same parameters as in Fig. 6. Both bounded and unbounded rays (solid lines) are shown. Black (V^-) and white (V^+) small circles denote the stationary points (corresponding to vortices) of opposite topological charge. Crosses (S) denote saddle points. The vortices are attractors for equiphase lines (dashed lines). The equiphase lines can join only vortices of opposite "charge."

pological charge to each vortex, and the equal-phase contours can join only the vortices with different charge (cf., e.g., [36]).

It is visible in Fig. 8 that the vortices form attractive basins for equiphase curves in certain ranges of phase values. There are rays that start initially very close to each other but one of them just goes without rounding a vortex, while the other one flows round it. It might be expected that the phase relation along these two rays is completely broken after rounding the vortex by one of them. This is not the case, however, since the change of phase after rounding the vortex is equal to an integer multiple of 2π.

C. Bounded structures of the flux

The apparently void island seen in Fig. 6 is displayed again in Fig. 9 but with the bounded rays, equiphase curves, and stationary points. It is clear that the island is actually not "void"; the solutions of the Maxwell equations show that the field intensities and the Poynting vector do not vanish and the wave-optical rays exist. The rays form, however, closed loops rather than unbounded curves.

Thus the "void" island is full of bounded, periodic trajectories, and plenty of stationary points, and is contained as a
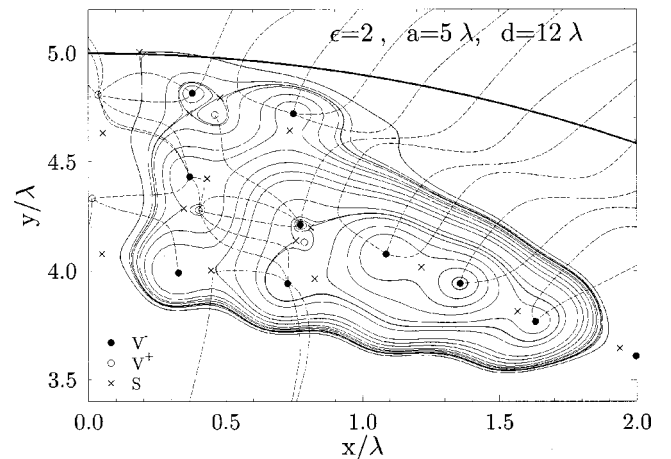
FIG. 9. Detailed structure of the flow in the void region of Fig. 6. Nested families of bounded rays are shown.
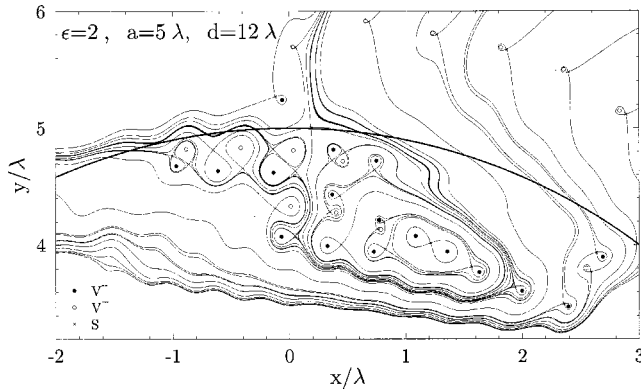
FIG. 10. Collection of all separatrices for an upper part of the cylindrical lens of Fig. 6. The lens is illuminated by a point source.

FIG. 11. Separatrices and equiphase lines for the isolated vortex saddle points pair. The same system as in the four previous figures.

whole within a large-scale periodic ray. Some vortices tend to group in pairs of stationary points with opposite topological charges, such pairs are assisted by pairs of saddle points. However, some single vortices are present as well so that total topological charge of the island is nonzero.

D. Ray separatrices

The plethora of wave-optical rays shown in Figs. 8 and 9 seem to avoid the stationary points, especially the saddle points. There are, however, some special rays that asymptotically approach the saddle points. These rays separate flows of different kinds. In the theory of dynamical systems [35] they are called separatrices. The separatrices can reach the saddle points for infinite values of the "pseudotime" τ. Two or more such separatrices that approach a single saddle point seem to intersect each other. They are in fact disconnected and there is no single dynamical trajectory passing through a saddle point, which could be obtained by integration of Eq. (12). Indeed two or three independent integrations of this equation are needed to obtain the full collection of ray separatrices attached to saddle points (three for unbounded ray separatrices and two for bounded). They have to start from points slightly displaced from the saddle points and one has to integrate both forward and backward in τ. The shape of any remaining ray is determined by two separatrices embracing it. Like all the other rays, the ray separatrices do not cross each other so that they can meet at one saddle point only (at $\tau = \pm \infty$).

All ray separatrices and stationary points that have been found in a region close to the boundary of the cylinder are shown in Fig. 10. This figure as well as Figs. 8 and 9 show that every saddle point can be associated with the corresponding vortex point. Not all data presented in Fig. 7 seems to confirm this property. However, this property is true; only due to the scale of the figure some vortex points and saddle points overlap. Figure 11 shows the vortex and saddle points together with equiphase lines and separatrices for the most right-hand vortex dot of Fig. 7. This figure looks almost identical to Fig. 11 of [17] that was considered as a generic example of a wave edge dislocation. Our discussion shows that such simple pattern of the energy flow may occur only in the vicinity of an isolated vortex point—saddle point pair.
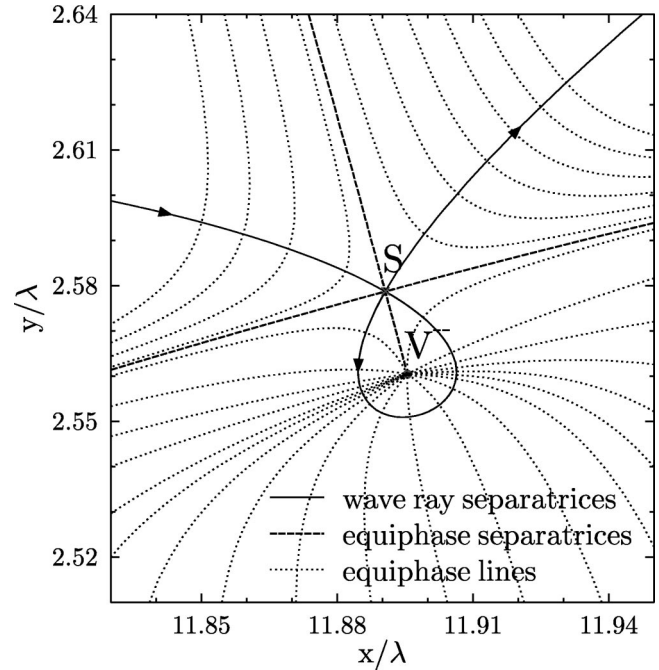
In addition to the light ray separatrices and equiphase lines this figure shows an object—equiphase separatrices. These equiphase separatrices determine boundary for different basins of the equiphase lines. This example shows that the saddle point, similarly as for the ray separatrices, is also a meeting point for the equiphase separatrices.

The following subsection discusses the equiphase separatrices in a region with many stationary points.

The number and location of stationary points is not an intrinsic property of the cylinder lens. It depends on the entire optical system that includes the sources of radiation. By moving the point source one can change the position of those points, hence the form of separatrices, which, in turn, changes the shape of the rays.

E. Equiphase separatrices

The equiphase contours can be divided into different classes by the equiphase separatrices. The equiphase lines and separatrices play a similar role to the wave rays and ray separatrices that characterize the light flow. An example of equiphase separatrices (bold dashed lines) with background of ray separatrices (thin lines) is shown in Fig. 12.

All equiphase separatrices are obtained integrating Eq. (14) in the forward and backward directions of τ, starting tfrom two points displaced infinitesimally in opposite directions from the saddle points. This way four equiphase separatrices attached to each saddle point can be found. The procedure is similar to that used in the case of ray separatrices.

These equiphase separatrices extend either to the neighboring vortex points or to the points on the optical axes $y = 0$. The end points on the optical axis can lie to the right of the light source at $x > x_0$ or, for equiphase lines encompassing the light source, at $x < x_0$.
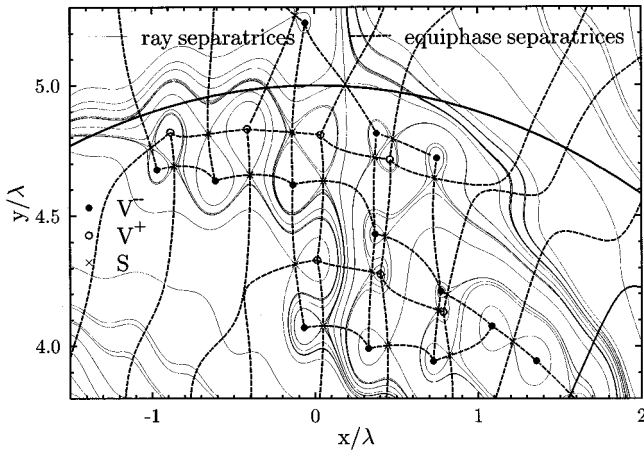
FIG. 12. Equiphase and ray separatrices in the multistationary points region. The same parameters as in the last figures.

The equiphase lines are always staying in the corresponding basins enclosed by the equiphase separatrices. They can extend either between the vortex points of opposite charge, or between the two points on the optical axis placed on the two sides of the source. The second case occur, for example, for equiphase circles surrounding the source in its vicinity.

F. Fixed points for the large cylinder

On having obtained the necessary experience by analyzing small cylinders we can reconsider the light propagating along a bigger system, to the one presented in Figs. 1, 2, and 5 (radius a equal to 15λ). The number of fixed points rapidly grows with the radius. In the upper half-plane displayed in Fig. 13, the number of stationary points is larger than 3000. Most of the singularities are concentrated in the annulus near the surface of the cylinder. In addition, there is a family of fixed points along the rim of the focused bundle of rays, as shown in Fig. 14. There is a clear correspondence between the positions of (groups of) stationary points in Fig. 13 and the form of the rays from Fig. 5. Also, the irregularities in the rays near the "entrance" (front) surface and "departure" surface of the cylinder in Fig. 2 are evidently connected with the region in which there is plenty of stationary points. The stationary points close to the optical axis in Fig. 13 enter
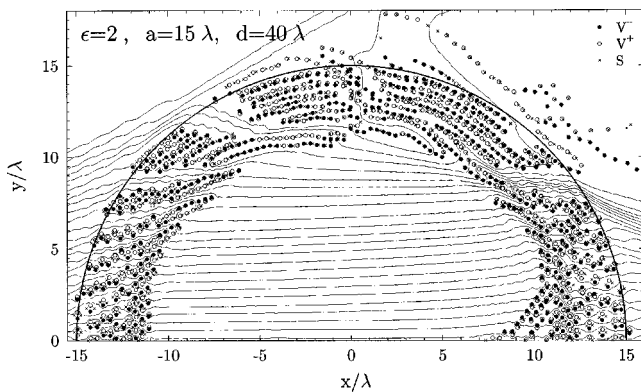
FIG. 13. All stationary points and their influence on the flow of the rays for a larger lens for the set of parameters of Figs. 2 and 5.
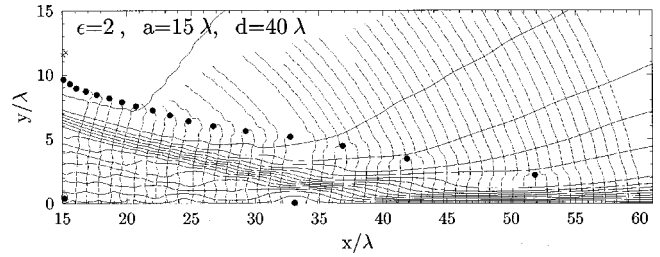
FIG. 14. Details of the structure of rays, equal-phase contours, and stationary points in the focal region; parameters are the same as in Figs. 2 and 5.

deeper towards the center of the cylinder and may thus be associated with a cusp of a caustic (compare Fig. 17 below). It is interesting that the stationary points are present on the optical axis as well, but there are no such points close to the position of the image of the source (see Fig. 14). At the image distance the stationary point is moved out of the axis.

As in the case of the smaller lens, the shapes of rays propagating through the optical system are determined by separatrices. The number of separatrices is very large and it does not seem useful to show them all. Their shape is similar to that shown for the smaller system. The loop part of most of them is of very small size, such that only one vortex point is included. There are, however, separatrices with large loops embracing several tens of stationary points as well as many bounded "internal" separatrices. Figure 15 presents those largest separatrices located at the top of the cylindrical surface. It is interesting to notice that, as in the case of smaller separatrices (Figs. 8–10), the large ones can form pairs with opposite vorticity of members of the pair.

V. RAY STRUCTURE AND FIXED POINTS FOR GAUSSIAN BEAMS

It has been observed by Karman and co-workers [19,18], that the structure of stationary points (phase singularities in his language) is strongly dependent on the type of source. In particular, they investigated in detail (both theoretically and experimentally) the case of a truncated Gaussian-beam illumination and the light structure in the focal region. One of their conclusions was that both the "creation" and "annihilation" of phase singularities can happen when proceeding from uniform to Gaussian illumination.

Let us now consider the case of the Gaussian-beam illu-
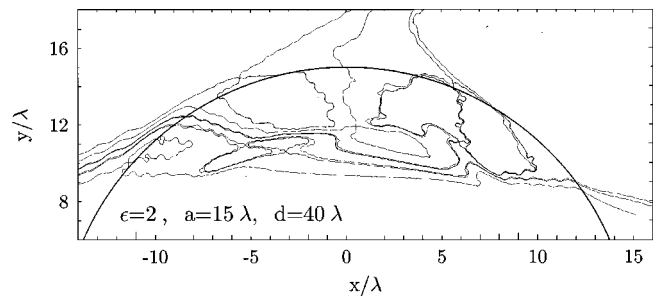
FIG. 15. Selected large-scale separatrices for the same system as in Fig. 5.
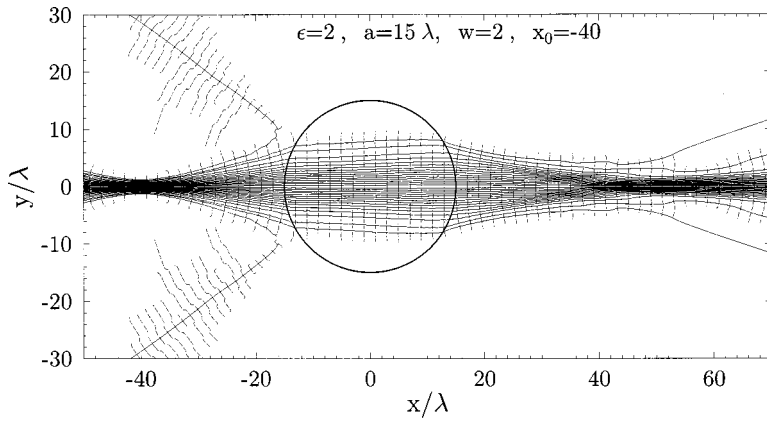
FIG. 16. Wave-optical rays and equal-phase contours for the Gaussian-beam illumination. The parameters are $a=15\lambda$, $\epsilon=2$, $w=2$.

mination. This can be a good model for light beams produced by many laser sources. In order to find out effects not visible in the case of point source and plane wave, the width w of the Gaussian beam cannot be either too large or too small. Indeed, if w were too large, the whole picture would be very similar to the case of the plane-wave illumination. If w were too small, the beam would spread out very fast resembling the point source pattern. But for an intermediate value of w, i.e., $\lambda r_0/(2a)<w<a$, the entire incident beam passes through the cylinder. A large portion of the scattered light stays outside the incident beam and, therefore, can be visible. The general pattern of the light scattered by the cylinder, including the rays and equal-phase contours, is shown in Fig. 16. The parameters of the position of the source and of the lens are the same as in Fig. 2. The light rays are started to keep equal fluxes between the subsequent lines. Comparing Fig. 16 with Fig. 2 we observe that the rays flow in a very regular, smooth way while the equal-phase contours inside the beam resemble those usually drawn for Gaussian beams. Most of them are terminated just out of the bundle of the rays of Fig. 16 since the intensity falls off exponentially and the right-hand side of Eq. (14) becomes extremely small.

In Fig. 16, one very distinguished feature is present. Two reflected rays appear, scattered at large angles. In the case of the other two sources considered in this paper, these large-angle scattered rays are hidden due to the overwhelming contribution of the incident beams. But the incident Gaussian
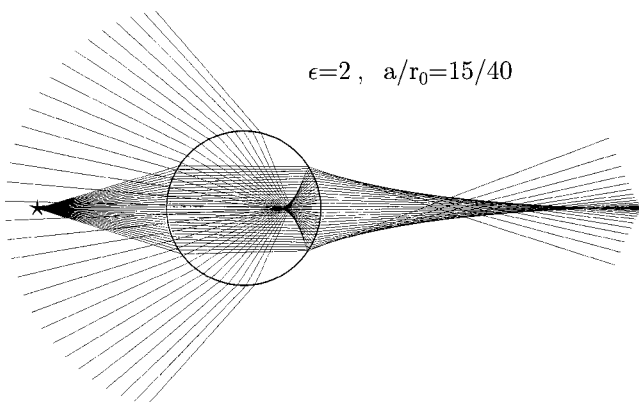
fields decay rapidly thus making possible the clear appearance of the reflected rays. The reflected rays shown in Fig. 16 correspond to a multiple-reflected geometro-optical ray contributing to the rainbow, as can be seen by comparison with geometrical-optics drawing of Fig. 17.

The smooth and regular flow of rays in the case of the Gaussian beam does not mean that there are no stationary points. They are, however, located outside the dominant part of the beam, cf. Fig. 18. A part of them bounds the beam before it enters the cylinder. There is an interesting oscillatory structure in the vicinity of the reflected ray. Lots of fixed points are present within the cylinder outside the beam and it seems that behind the lens and close to the optical axis there is a similar group of these points as in the other illuminations shown in Fig. 14. One cannot, however, consider these results to be complete.

VI. INTENSITY AND PHASE PROFILES ALONG THE OPTICAL AXIS

Our approach enables us to show the properties of both the intensity and phase of the fields (which are often discussed in a similar context) along the optical axis. The phase is specified as $\Phi=\arg(E_z)$.

For the case of the point source, Fig. 19, the intensity is a very rapidly oscillating function of position along the axis. The change in the oscillation pattern close to the boundaries of the cylinder clearly correspond to the structure of stationary points shown in Fig. 13. A similar change of pattern is evident in the position dependence of the phase, which varies rapidly in the same regions. Beyond the cylinder, we have

FIG. 17. Geometric-optics rays starting at a point source. The rays that had been internally reflected one time are visible including those contributing to the rainbow.
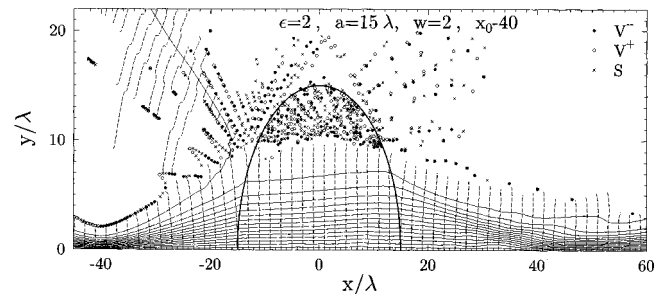
FIG. 18. Stationary points of the flow for the Gaussian-beam illumination. All the parameters are as in Fig. 15.
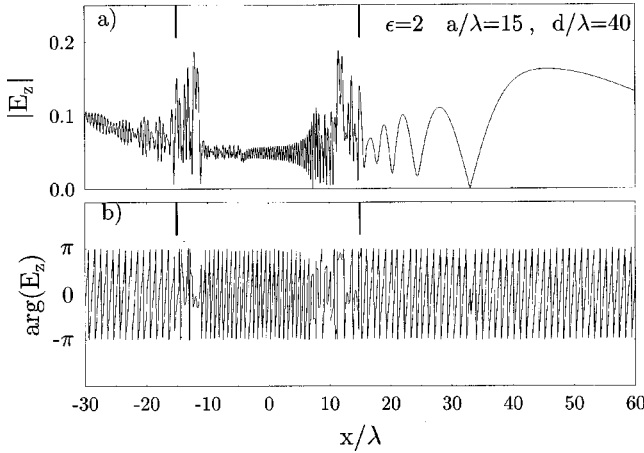
FIG. 19. Intensity and phase along the optical axis for the point source case.

FIG. 21. (a) Wave-optical rays for radiation from two point sources scattered by the cylindrical lens. Formation of inverted image by the enlarged concentration of rays is shown. (b) The same image formation according to the geometrical optics.

found only one point of the phase anomaly close to the point $x/\lambda \sim 33$ (see Fig. 14 for a comparison). To our surprise, we have not detected any phase jump close to the image region.

For the case of Gaussian beam, the analogous intensity oscillations are much smaller as shown in Fig. 20. The behavior of phase is very regular except the small irregularities at $x/\lambda \sim 7$ that one may possibly associate with the geometro-optical cusp occurring in Fig. 17. Again, there is no phase jump either at the source or at the image position.

VII. IMAGE FORMATION OF EXTENDED OBJECTS IN WAVE OPTICS

We have stressed several times that the wave-optical rays as defined in this paper cannot intersect. But then the follow-

FIG. 20. (a) Intensity of the field for the Gaussian-beam illumination along the optical axis. (b) Phase distribution along the optical axis for the Gaussian-beam illumination.

ing question arises: how is it possible to get the inverted images of objects, which is usually obtained in the geometrical optics by a construction that requires the crossing of rays? Another important question is, how to get the wave-optical picture of multiple reflection inside the cylinder? The former one will be discussed in this section, while the latter in the following one.

To answer the first question in the simplest way, we discuss the wave-optical rays from two point sources located in the vicinity of the cylinder. Let us for a moment assume that the sources are coherent—they oscillate with the same frequency and the phase difference is fixed. The total fields are superpositions of the fields irradiated by each source, and the interference effects clearly have to be present. The rays must not be, of course, simply "added," but should be obtained from the total electric and magnetic fields and the corresponding Poynting vector.

The flow of the wave-optical rays case is displayed in Fig. 21(a). The rays start at both the emission points. If there was no lensing cylinder, the density of rays would form interference fringes around the system. The cylinder itself gives rise to the image of the sources in a very peculiar way. The rays starting at the more distant source do not have any chance to reach the cylinder at all. Only the rays starting at the closer source enter the cylindrical lens. In spite of this fact, two distinct ray concentration spots are apparent corresponding the source images as is clear by comparing with the geometrical construction shown beneath [Fig. 21(b)]. Thus, the information on the second source is "recorded" and contained in the rays originating at the closer one. The visibility of images of the sources becomes better for larger cylinder size as it gathers more radiation rays. Thus the contrast be-
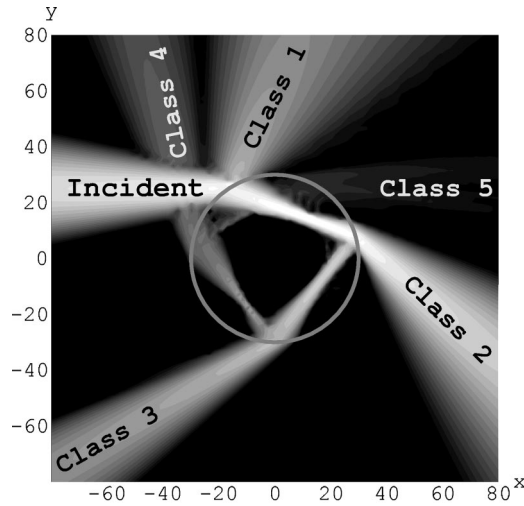
FIG. 22. Shaded contour plot of constant modulus of the Poynting vector ($\log_{10}|\mathbf{S}|$) (light intensity shades; contours themselves are removed) for the noncentral Gaussian-beam illumination. Multiple refraction and reflections are apparent. The position of the waist of the beam (units of λ) is $x_0 = 0$, $y_0 = 25$, the width of the beam $w = 4$, the radius of the cylinder $a/\lambda = 30$.

FIG. 23. Wave-optical rays for the same illumination and parameters as in Fig. 22. It is clear that the rays do not intersect. The rays corresponding to the double internal reflection are formed—inside the lens—by the ''circulating'' (periodic) rays, which are thus necessary to obtain the full picture of scattering with multiple reflections.

tween the image spots and the surrounding regions is better. Figure 21(a) has been drawn for zero difference between phases of the two sources. In the case of nonzero difference, the individual rays could look differently, but the concentration spots would stay at the same places so that the coherence of two sources assumed above does not matter.

VIII. MULTIPLE-REFLECTED AND REFRACTED RAYS

To address the second important question posed above we consider multiple reflections inside the cylinder. In geometrical optics such multiple reflections obviously lead to the (multiple) ray intersections. Now, our wave-optical rays cannot cross. To solve this puzzle, let us consider a Gaussian beam entering the cylindrical lens noncentrally. Figure 22 shows the modulus of the Poynting vector (not yet the rays) inside and close to the lens. The shades of gray ranging from white to black are proportional to $\log|\mathbf{S}|$ and cover the range of 40 dB of relative intensities to highlight the small intensities of multiple-reflected beams.

The presented exact solution shows in a natural way the multiple reflection and transmission (corresponding to Class 1 - Class 5 of rays in [20]). There is no need for any extra assumptions or constructions. Parts of the reflected beam after two and three internal reflections are very important as they contribute to the rainbow. Every reflection takes into account the curvature of the reflecting cylindrical surface including the focusing properties (such as in a composite optical system). However, Fig. 22 itself does not yet solve the ''intersection'' puzzle.

Only a picture of wave-optical rays themselves can lead to the solution. It is shown in Fig. 23, again for the Gaussian-beam illumination entering the lens from the left-hand side with a nonzero impact parameter. In the entering bundle of rays there is a splitting into sub-bundles corresponding to
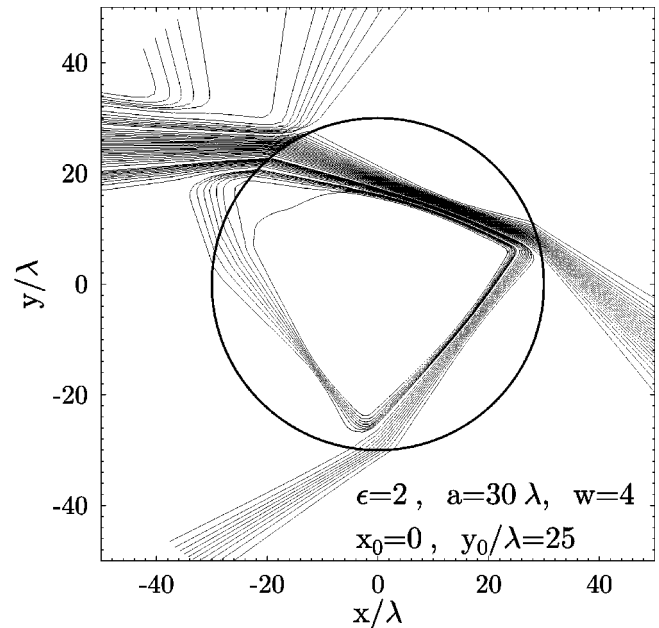
direct reflection, direct transmission, as well as to single and double internal reflections. The picture is not complete, however, unless we draw the ''circulating'' rays that do not originate in the entering bundle. The bundle of rays of Class 3 (cf. [20]) consists of the circulating sub-bundle and a peripheral part of the incident bundle. The fact that these two parts fit so well is truly astonishing. These two examples show that even in the situation in which we could expect the crossing of trajectories, they find their way to avoid any intersection.

IX. FINAL REMARKS

This discussion shows how the solutions of Maxwell equations for various electromagnetic radiation beam problems or external source problem and their scattering by a dielectric cylindrical lens may illustrate all optical effects involving light propagation. It is possible to account for reflections, refractions, focusing and image formation, appearance of caustics and foci, waves' interference and diffraction, etc. Usually such effects are treated in the approximate theories referring either to geometrical or diffractive optics. The long history of research in optics resulted in well developed and understood accurate analytical methods and the quality of optical instruments is the best proof of the value of optical theories. However, I do believe that the present discussion using explicit solutions for the fields has revealed interesting properties of classical electromagnetic radiation.

Taking these findings into account, we may conclude that the concept of rays is still very well defined in the full wave theory. What is more, these rays may be used to find the images of objects formed by optical devices. The images are

regions in space where the density of rays becomes large. Also, we argue that the ray concept is not less useful in the full Maxwell theory than in the geometrical optics. The images of objects provided by optical devices can be rigorously obtained by tracing the rays being integral curves of the Poynting vector. It is to be noted that the tracing of "physical" rays, that is, the integration of the Poynting vector field, must be performed with extreme care. Indeed, the rays are not segments of straight lines, and they can even be quite erratic. This is obviously connected with the properties of the phase of electromagnetic field that can be an extremely complicated function of a position in space.

It is to be noted that the geometrical rays are self-determined and can be plotted without any knowledge of the fields. In fact, they can be specified with the help of a few simple rules and equations even for multicomponent sources. On the other hand, the wave rays discussed in this paper are not self-defined and require first the solution for the field in a given problem. Only after these fields are known the wave rays can be determined. Thus, the wave rays allow to represent and illustrate in full richness the wave properties of light and can be compared to the properties of geometrical rays.

Concluding this discussion one can pose some interesting and fundamental questions to be addressed in the future. In particular, when the rays are not straight lines but can become quite complicated curves, what is the meaning of the "optical path" in wave optics? Moreover, how can we formulate a wave-optical version of the Fermat principle, so that the curves of energy flow would provide the solution to a corresponding variational problem? Besides, we believe that the above discussion can be useful for investigations of more complicated systems, as, e.g., a dielectric sphere and real electromagnetic fields requiring 3D analysis. In fact, even a dielectric cylinder would lead to 3D problems if the incident beams were finite in the two transverse directions.

[1] M. Born and E. Wolf, *Principles of Optics* (Cambridge University Press, Cambridge, 1998).

[2] A. Sommerfeld, *Optics* (Academic Press, New York, 1954).

[3] R. K. Luneburg, *Mathematical Theory of Optics*, Polish translation (PWN-Polish Scientific, Warsaw, 1995).

[4] E. Hecht, *Optics*, 3rd ed. (Addison-Wesley, Amsterdam, 1998).

[5] J. F. Nye, *Natural Focusing and Fine Structure of Light* (Institute of Physics Publishing, Bristol, 1999).

[6] A. Sommerfeld and I. Runge, Ann. Phys. (Leipzig) **35**, 277 (1911).

[7] E. Madelung, Z. Phys. **40**, 322 (1926).

[8] L. Landau and E. Lifshitz, *The Classical Theory of Fields* (PWN-Polish Scientific, Warsaw, 1958).

[9] B. Richards and E. Wolf, Proc. R. Soc. London, Ser. A **253**, 358 (1959).

[10] A. Boivin and E. Wolf, Phys. Rev. **138**, B1561 (1965).

[11] A. Boivin, J. Dow, and E. Wolf, J. Opt. Soc. Am. **57**, 1171 (1967).

[12] D. Jackson, *Classical Electrodynamics* (PWN-Polish Scientific, Warsaw, 1982).

[13] J. J. Stamnes, *Waves in Focal Regions* (Institute of Physics Publishing, Bristol, 1986).

[14] T. Pearcey, Philos. Mag. **37**, 311 (1947).

[15] M. V. Berry and C. Upstill, in *Progress in Optics*, edited by E. Wolf, Vol. XVIII (1980), p. 259.

[16] M. V. Berry, in *Physics of Defects*, Proceedings of the Les Houches Summer School, Session 35, edited by R. Balian, L. Kléman, and J-P. Poirier (North Holland, Amsterdam, 1981), pp. 454–543.

[17] J. F. Nye and M. V. Berry, Proc. R. Soc. London, Ser. B **336**, 165 (1974).

[18] G. P. Karman, M. W. Beijersbergen, A. van Duijl, D. Bouw-meester, and J. P. Woerdman, J. Opt. Soc. Am. A **15**, 884 (1998).

[19] G. P. Karman and J. P. Woerdman, J. Opt. Soc. Am. A **15**, 2862 (1998).

[20] H. M. Nussenzveig, Sci. Am. **236**, 116 (1977).

[21] H. M. Nussenzveig, *Diffraction Effects in Semiclassical Scattering* (Cambridge University Press, Cambridge, 1992).

[22] V. Khare and H. M. Nussenzveig, Phys. Rev. Lett. **33**, 973 (1974).

[23] H. M. Nussenzveig, J. Math. Phys. **10**, 82 (1969).

[24] Lord Rayleigh, Philos. Mag. **36**, 365 (1918); **12**, 81 (1881); John William Strutt-Baron Rayleigh *Scientific Papers* (Cambridge University Press, Cambridge, 1899), Vol. 1, p. 533.

[25] D. S. Jones, *Acoustic and Electromagnetic Waves* (Clarendon Press, Oxford 1986).

[26] S. Kozaki, J. Appl. Phys. **53**, 7195 (1981).

[27] E. Zimmermann, R. Dändliker, N. Souli, and B. Krattiger, J. Opt. Soc. Am. A **12**, 398 (1995).

[28] J. P. Barton, J. Opt. Soc. Am. A **16**, 160 (1999).

[29] W. Żakowicz and M. Janowicz, Phys. Rev. A **62**, 013820 (2000).

[30] W. Braunbek and G. Laukien, Optik (Stuttgart) **9**, 174 (1952).

[31] J. O. Hirschfelder and K. T. Tang, J. Chem. Phys. **65**, 470 (1976).

[32] J. F. Nye, J. Mod. Opt. **38**, 743 (1991).

[33] D. E. Amos, amos.lib, http://www.netlib.org.

[34] M. V. Berry, J. F. Nye, and F. J. Wright, Philos. Trans. R. Soc. London **291**, 453 (1979).

[35] V. I. Arnold, *Ordinary Differential Equations* (PWN-Polish Scientific, Warsaw, 1975).

[36] I. Freund and N. Shvartsman, Phys. Rev. A **50**, 5164 (1994).